Research on an Automatic Tracking Strategy Based on CCD Image Sensor in Micromanipulation

XIN YIN [ID] [1], GUONAN JIANG[1], AND SHIDONG SONG[2]
[1]Tianjin Key Laboratory of Wireless Mobile Communications and Power Transmission, Tianjin Normal University, Tianjin 300387, China
[2]School of Environmental and Chemical Engineering, Tianjin Polytechnic University, Tianjin 300387, China

Corresponding authors: Xin Yin (yinxin1025@126.com) and Shidong Song (songshidong@sina.com)

ABSTRACT In this paper, an automatic tracking strategy based on a CCD image sensor is proposed to achieve the real-time tracking of embryonic cells with the MR-6 micromanipulator. The optical characteristics of the micro-vision sensor are systematically studied. Dark field is formed by the optical microscope imaging principle under the low rate objective lens. The global information of the embryo cells is tracked automatically using the improved Hungarian algorithm, so that the motion parameters of the batch of embryo cells and the interested area can be obtained. Then, the detailed information of the interested area is obtained in the bright field using the automatic conversation device. In addition, the feasibility of the algorithm is further verified by automatic experimental research.

INDEX TERMS CCD image sensor, optical transfer function, micromanipulation, Hungarian algorithm.

I. INTRODUCTION

Micro vision sensor has been played an important role in micromanipulation. The most of the current research is based on static passive sensors [1], [2], which cannot change the resolution of images [3], [4]. It is of significant importance to track the trajectories of embryonic cells and study their movement features during the process of embryonic development, which help the medical researchers to treat highly diffusive diseases and carry out the corresponding pharmacology studies [5]–[10]. Therefore, the real-time tracking and analysis of the embryonic cells under the different resolution has attracted much attention in the field of life science [11]–[14]. Amariglio indirectly evaluates the motion features of individual cell by establishing colony scratches for cells [15]. This method is simple, but cannot be effective to track the trend of overall movement for embryonic cells. So far, the study on tracking the targets in real time at different resolutions is really rare.

In this work, with a view of the real-time tracking, a tracking strategy based on CCD image sensor is proposed, which makes it feasible to obtain multi-scale information in the target tracking process. The MR-6 micromanipulation robot system is applied for the migration tracking and analysis of embryo cells. The multi-scale automatic tracking strategy and the optical characteristics of the microsystem are systematically studied. The organization of this paper is as follows. A tracking strategy based on CCD image sensor in batch embryos is introduced in Section II. Section III describes the related automatic experiment. Conclusions are given in Section IV.

II. THE AUTOMATIC TRACKING STRATEGY BASED ON CCD IMAGE SENSOR IN BATCH EMBRYOS

Because cell migration is occurred after the cell receiving the migration signal or feeling the concentration gradient of certain substances, the cell cluster is bound to have a consistent movement trend. At the same time, during the cell movement, the single cell repeats the motion of extending the synapse and pulling the rear cell to the forward. Observation and analysis of the process are conducive to understanding the mechanism of cell migration. During tracking the overall movement of the cell cluster, the morphology of the single embryo cell should be observed in real time. At the same time, in order to obtain the overall movement trend of the cell cluster, it is necessary to track the whole batch of embryo cells. Furthermore, considering the living characteristics of the embryonic cells, the tracking time should be as short as possible to strengthen the tracking calculation. In addition,

all the operations should be done automatically to reduce the workload of the experimenters.

However, there is often a tradeoff between the acquisition of the overall movement trend for the embryo cells and the observation of the delicate structure of single particle under high resolution. The increase in the visual field magnification will reduce the observable space and introduce the visual sampling error. On the other hand, the low magnification reduces the visual sampling error, but the effective image resolution of the target will be reduced as well. In addition, the dark field microenvironment uses the Tyndall optical effect to improve the contrast between the observed object and the background, which is beneficial for observing the moving objects but is bad for obtaining the details of the object. Therefore, in order to obtain the accurate movement trend of embryo cell cluster, it is preferable to observe the targets under the low magnification in dark field while to collect the morphology and structure of the single embryo cell under the high magnification in bright field. On the other hand, the automatic and real-time tracking of the batches of cells is also a difficult problem. At present, the commonly used tracking methods can be roughly divided into four kinds: the active contour based method [16]–[18], the region based method [19], the model based method [20], [21] and the feature based method [22]–[24]. The tracking algorithms of moving targets in microscopic images are different from that of the macro target since the deletion and fragmentation of cell edge fragments, and the adhesion and overlap of cells are large challenges [25]–[27].

During the tracking of embryo cells, the overall movement trend of the cell cluster and the details of the single cell are difficult to obtain at the same time. Thus; the dark field of view is formed by using the optical microscope imaging principle under the low rate objective lens, and the embryo cells are automatically tracked with the improved Hungarian algorithm. The global information of the cell is used to obtain the motion parameters of the batch embryo cells and identify the regions of interest, so as to realize the automation for the analysis on the overall movement trend of the embryonic cells. At the same time, the time slice is allocated for different regions of interest (usually more than 1 minutes). The automatic switching between the dark field and the bright field and the area of interest of the time film can be achieved. The automatic transformation and focusing is carried out by the MR-6 micromanipulation robot. The simultaneous acquisition of the global view and the region of interest for embryonic cells can be achieved. The algorithm flow is shown in Figure 1.

A. IMAGE ACQUISITION IN DARK FIELD OF VIEW

In order to achieve the rapid and accurate tracking as well as the location of multiple cells, it is necessary to improve the contrast between embryonic cell and background. During the light propagation, when the irradiated particles are smaller than the wavelength of incident light, the light wave will
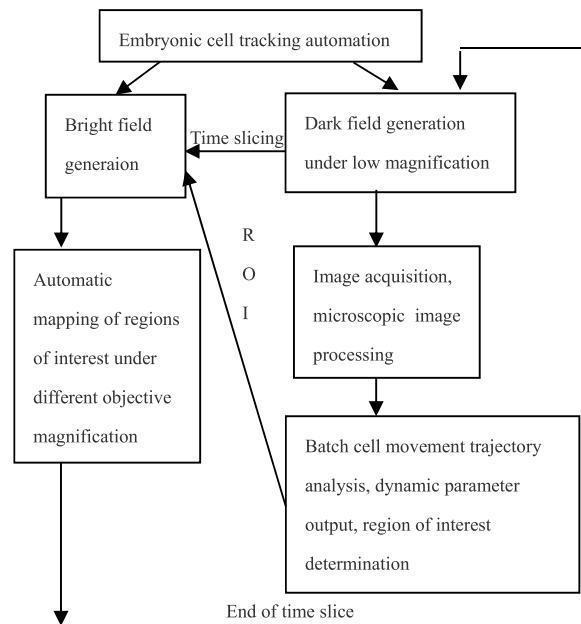

FIGURE 1. Algorithm flow of the tracking strategy based on CCD image sensor in batch embryos.

surround the particles and radiate the scattered light around them. Therefore, according to the principle of microscope optical imaging, the dark field of view is used to complete the global microscopic images for the migration and tracking of low-rate embryo cells.

B. TRACKING STRATEGY FOR OBTAINING CELL MOTION INFORMATION BASED ON THE IMPROVED HUNGARIAN ALGORITHM

Cell matching is the key step for the migration and tracking of batch cells. This paper proposes a tracking strategy based on the improved Hungarian algorithm [28]–[30].

1) OBTAINING THE POINT SPREAD FUNCTION IN THE PROCESS OF IMAGE IMAGING

Point spread function (PSF) smoothing model is used to realize the PSF scale space under different scales by convolution. PSF is an index used to describe the object space and image space in optical sensor system. Deconvolution of the images, captured by the microscope and the object, is used to get the PSF.

2) REPRESENTATION OF PSF SCALES SPACE

As shown in formula one, the scale space of an image $L(x, y, \sigma)$ is defined as the convolution of a variable scale PSF function $PSF(x, y, \sigma)$ and the original image $f(x, y)$.

$$L(x, y, \sigma) = PSF(x, y, \sigma) * f(x, y) \qquad (1)$$

Where σ is a scale spatial factor. The smaller the σ value, the smaller the image is smoothed out, and the smaller the corresponding scale.

3) CONSTRUCTING PSF PYRAMID AND GETTING PSF DIFFERENCE IMAGE

The pyramid model of image refers to the model composed of a series of images of different sizes, from large to small, from bottom to top, by continuously reducing the order of the original image to sample. The original image is the first layer. PSF difference image is obtained with the formula two.

$$D(x, y, \sigma) = (G(x, y, k\sigma) - G(x, y, \sigma)) * f(x, y) \quad (2)$$

4) DETECTION THE KEY POINT

The key points comprise the local extremum points of PSF difference space (PDS).

Descriptors with Scale-invariant feature transform(STFT) is used in detecting the key point. SIFT is a computer vision algorithm for detecting and describing local features of images. It searches for extreme points in spatial scale and extracts their position, scale and rotation invariants. Description and detection of local image features can help identify objects. SIFT features are based on interest points of some local appearances of objects and are independent of image size and rotation. Thus, the tolerance of light, noise and micro angle changes is relatively high. Based on these characteristics, it is highly significant and relatively easy to retrieve the SIFT features. Based on a large number of feature databases, it is easy to identify objects and rarely misrecognize them. SIFT features the large amount of information and is suitable for fast and accurate matching in massive data. Combining with the optical characteristics of microscope, an improved Hungarian algorithm is then proposed.

The initial detection of the key points is accomplished by comparing the adjacent two layers of images in the same group of PDS. In order to find the extremum of PDS function, each pixel is compared with all its adjacent points to see if it is larger or smaller than the adjacent points in its image domain and scale domain. The intermediate detection point is compared with its eight adjacent points of the same scale and the 9*2 points related to the upper and lower adjacent scales, which are 26 points in total, to ensure that the extreme points are detected in both the scale space and the two-dimensional image space.

5) KEY POINT FEATURE DESCRIPTION

In order to determine the descriptor rotation invariant, it is necessary to assign a reference direction to each key point by using the local features of the image. The stability direction of local structure is obtained using image gradient method. For the key points detected in the PFS pyramid, the gradient and direction distribution characteristics of pixels in the neighborhood window of the Gauss pyramid image 3 are collected. The modulus and direction of the gradient are as follows:

$$m(x, y) = \sqrt{(L(x+1, y) - L(x-1, y))^2 + (L(x, y+1) - L(x, y-1))^2}$$

$$\theta(x, y) = tan^{-1}(\frac{L(x, y+1) - L(x, y-1)}{L(x+1, y) - L(x-1, y)}) \quad (3)$$

Through these steps, each key point has information on location, scale and direction. The next step is to create a descriptor for each key point, using a set of vectors to describe the key point, so that it does not have all kinds of changes, such as lighting changes, perspective changes, and so on. This descriptor includes not only the key points, but also the pixels contributing to them around the key points. The descriptor should have higher uniqueness in order to improve the probability of correct matching of feature points.

6) MATCH THE KEY POINT IN EACH FRAME USING THE HUNGARIAN ALGORITHM

Hungarian algorithm is based on a Euclidean distances matrix that is obtained from the SIFT descriptor. The size of matrix can vary over time according to the objects appeared and disappeared. The Hungarian algorithm achieves target matching between consecutive frames, and is used to identify vanishing targets and emerging targets in automatic tracking.

Hungarian algorithm steps are as follows:

Step 0: Construct a cost matrix of n * m. n is the number of key points in one frame and M is the number of key points in the next adjacent frame. If the number of columns of the matrix is not consistent with the number of rows, it is necessary to extend the matrix to k = min (n, m).

Step 1: Finds out the minimum value of every row in the matrix and subtracts the minimum value from all values.

Step 2: Find the value of zero in the matrix. Find the value of zero in the cost matrix. If there is no asterisked zero in the rows and columns, add an asterisk to the zero in the position.

Step 3: Overlay each column with an asterisk of zero, if there is a K column overwritten, then you can get the best match, otherwise Step4;

Step 4: Looking for the uncovered 0 in the matrix, marking it as 0', if there is no other * 0 in the row of 0', proceed directly to Step 5, otherwise cover the row of 0', do not cover the column of * 0 in the row; if the uncovered area does not contain 0 in the matrix, find the minimum value in the uncovered area, proceed to Step 6;

Step 5: Construct a series of optional 0's and * 0 as follows, let Z0 denote 0'in the uncovered region of Step 4, Z1 denote * 0 in the column where Z0 is, Z2 denote '' in the row where Z1 is, until there is no other * 0 in the column where 0' above is, then remove all * 0's * and replace all '' in the matrix with *. Cover the line back to Step3;

Step 6: Add the minimum value found in Step 4 to each value of row coverage, subtract the minimum value for each column of the uncovered area, and return Step 4.

Step 7: Find the best match, if the position of C (I, j) is * 0, then the corresponding row and column are the best match respectively.

If n is greater than m, no matching (n-k) cells end tracking. If n is less than m, no matching (m-k) cells are added to the next tracking object group.

2.3 Automatic acquisition of detail information on region of interest in microscopic images

According to the characteristics of the alignment axis of the microscope, the system realizes the automatic acquisition of the detail information on the region of interest under the low magnification in objective microscope image in the open field.

III. EXPERIMENTAL RESEARCHES ON AUTOMATICALLY TRACKING BATCH EMBRYO CELLS

Chicken has unique biological characteristics and thereby become an important model organism for many biological problems. The embryonic development of chicken can provide a lot of inspiration for researches on human and other model animals. In the automation experiment, the chicken embryo's intestinal embryo formation was used as the experimental research model, and the automation tracking method of embryo cell migration was applied to the migration tracking experiment for chicken embryo cell. The automation experiment of chicken embryo cell migration was carried out using the micromanipulation robot system to obtain the dynamic model of chicken embryo cell migration.

Cell images captured in the dark field of view have the characteristics of black background and prominent contour information. Compared with the light field microscopic image, the dark field microscopic image weakens the interference information of the background, so the target information can be clearer, which is helpful to observe the cell movement process, as shown in Fig.2.
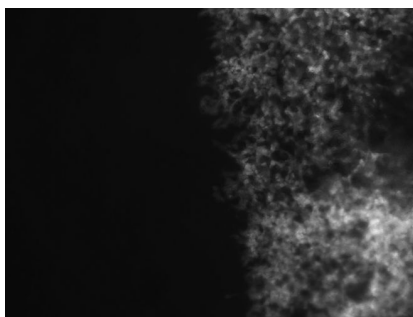

FIGURE 2. Chicken embryonic cell in the dark field of view.

The OLYMPUS IX71 inverted microscope with the halogen bulb of 12V100WHAL (PHILIPS7724) (IX2-ILL100 illumination column) was used to obtain the field of view diaphragm by adjusting the aperture to the smallest and the objective lens microneedle under 10 times focusing. After focusing, the microneedle is removed using the high-speed image recording system (GVMC01-BO5) which records the image produced by point light source. In order to further realize the automation of migration and tracking, the micro-manipulator is equipped with an automatic field-of-view conversion device and an automatic dimming device. The positions of the two devices in the micro-manipulator microscope are shown in Fig.3.

The parameters of 4- and 10-times eyepieces in the micro-operating system are analyzed and the suitable objective
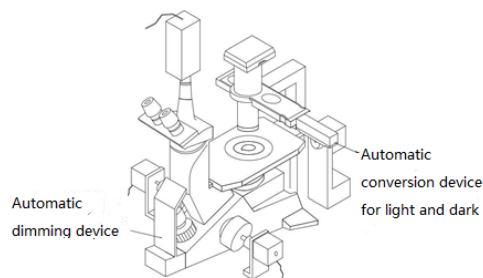

FIGURE 3. Mechanical structure of micro manipulation robot platform.

TABLE 1. The related parameters for ten-times objective.

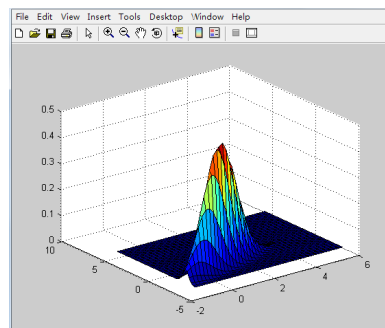| |
|---|
| $d_f = 195/(M+1) = 17.7$ |
| $d_i = d_f.M = 177.3$ |
| $f = d_i/(M+1) = 16.1$ |
| $\alpha = \arcsin(NA) = 14.5$ |
| $A = d_f \tan(\alpha) = 4.6$ |
| $\alpha' = \arctan(A/d_i) = 1.48$ |

FIGURE 4. Convolution kernel of PSF scale space.

is selected. The optical parameters of the 10-times objective are calculated. The magnification M of the 10 times objective is 10. The numerical aperture NA is 0.93. The wavelength of the system light source and the cut-off frequency of the digital imaging system, as well as the relative parameters of 10-times objective lens can be obtained by calculation, as shown in Table 1.

Similarly, 4-times of objective parameters can be calculated. Fig.4 is the convolution kernel of PSF scale space. In two-dimensional space; the contours of the surface generated by this formula are concentric circles with normal distribution from the center. The non-zero pixel convolution matrix is transformed with the original image. The value of each pixel is the weighted average of neighboring pixels. The value of the original pixel has the largest PSF distribution value and the largest weight. As the adjacent pixels are farther away from the original pixel, their sizes gradually reduce.
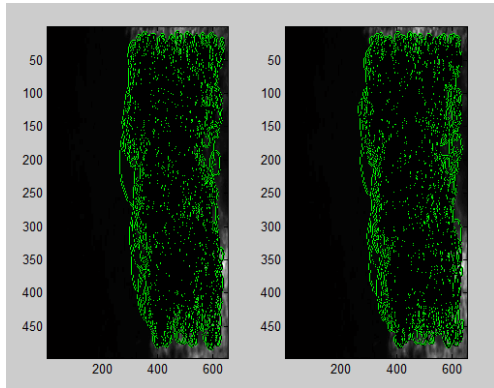
FIGURE 5. The Sift descriptors in the selected adjacent two images randomly.

FIGURE 6. The vector of descriptors in the second image.

This fuzzy process preserves the edge effect, which is better than other balanced fuzzy filters.

Fig.5 is the SIFT descriptors in the selected adjacent two images randomly. 1643 descriptors are obtained from the first image, and 1683 descriptors are obtained from the second image. Fig.6 is the vector of descriptors in the second image.

Then, the distance matrix is obtained and stored in a vector, whose size is 1643*1683.

The Hungarian algorithm realizes target matching between consecutive frames, which is shown as follows:

The distance matrix is gives as A[m,n], and the number of matched point is k, where k=min{m,n}.

If (k=m=n), then

$$A[k,k] = [1, 2, 3, 4, 2, 4; 4, 2, 1, 3, 3, 2; 2, 1, 2, 2, 4, 1;$$
$$2, 4, 1, 1, 2, 3; 2, 4, 1, 4, 1, 2; 1, 4, 2, 4, 3, 1];$$

$$\begin{matrix} 1 & 0 & 0 & 0 & 0 & 0 \\ 0 & 0 & 1 & 0 & 0 & 0 \\ 0 & 1 & 0 & 0 & 0 & 0 \\ 0 & 0 & 0 & 1 & 0 & 0 \\ 0 & 0 & 0 & 0 & 1 & 0 \\ 0 & 0 & 0 & 0 & 0 & 1 \end{matrix}$$

The matched target map is shown in Fig.7.

If k is less than n, it indicates that some traced targets is vanished. The experimental results are shown in Figure 8. Vector ff stores items that do not match.
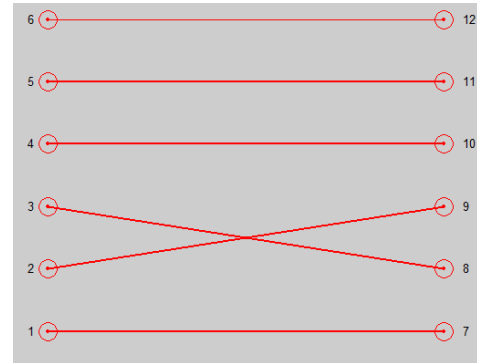

FIGURE 7. Matched target map.

FIGURE 8. Identify vanishing target.

If k is greater than n, it indicates that there are some new traced objects. The procedure is shown as follows:

$$A[m,n] = [1, 3, 3, 4, 2, 4, 1; 4, 2, 1, 3, 3, 2, 3; 2, 1, 2, 2, 4,$$
$$1, 4; 2, 4, 1, 1, 2, 3, 4; 2, 4, 1, 4, 1, 2, 3;$$
$$1, 4, 2, 4, 3, 1, 4]$$

$$A[k,k] = [1, 3, 3, 4, 2, 4; 4, 2, 1, 3, 3, 2; 2, 1, 2, 2, 4, 1;$$
$$2, 4, 1, 1, 2, 3; 2, 4, 1, 4, 1, 2; 1, 4, 2, 4, 3, 1];$$
$$ff = [1; 3; 4; 4; 3; 4],$$

where ff stands for the new traced objects.

Fig.9 shows the cell tracing process of the Adjacency frames in the multicellular tracking experiment.

The detail information acquisition process under high resolution is as follows. Firstly, the pixel space coordinates of the center point C(384, 288) are obtained according to the constant window of the microscopic image with the resolution of 768* 576. The region of interest is selected at low magnification. Each pixel is measured at about 2.996 microns under the quadratic objective. The distance at X and Y direction
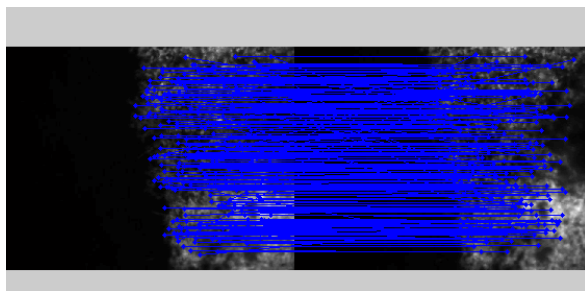
FIGURE 9. Tracked cell in image sequence.

from the center of the coordinate to the lower left corner of the selected area is obtained from formula four.

$$\begin{cases} SX = 2.996(384 - x1) \\ SY = 2.996(288 - y1) \end{cases} \quad (4)$$

Where x1 is the X axis coordinates and y1 is the Y axis coordinates of the Point A, which is the lower left corner of the selected area. According to the principle of distance invariance, the distance between the center point and the point in the lower left corner is invariable, so the micro-manipulation platform can move the corresponding distance at the X axis and Y axis directions according to the distance from the lower left corner to the image space coordinates. The lower left corner of the 4-times objective is moved to the center of the high-power objective, and the micro-manipulation platform is set to move to the right if the value of SX is positive or to the left if the value of SY is positive. Otherwise, the micro-manipulation platform moves upward if SY is positive, and the micro-manipulation platform moves downward, which enable the coordinates of the lower left corner to move to a high position. Then, according to the coordinates of point C (x2, y2), the distances between point C and point A at the X, Y axis directions are calculated respectively. Let SX1 be the distance difference between point A and point C at the X direction, and SY1 be the distance difference between point A and point C at the Y direction.

$$\begin{cases} SX1 = 2.996(x2 - x1) \\ SY1 = 2.996(y2 - y1) \end{cases} \quad (5)$$

The distance difference between point A and point C at the X and Y axis directions indicates the width and height of the selected area. The scanning range at the X and Y axis directions can be calculated in formula six, where s is the distance of each movement of the electric vehicle platform under the high magnification objective.

$$\begin{cases} SSx = X1/s \\ SSy = Y1/s \end{cases} \quad (6)$$

IV. CONCLUSION
Aiming at the challenge that the global view of multi-target and the detail information of single target cannot be obtained

simultaneously during micro-target tracking, a tracking strategy based on CCD image sensor is proposed. The global information of the embryo cells can be tracked automatically with Hungarian algorithm. Key points are established based on optical scale space and SIFT descriptor .Hungarian algorithm is used to identify vanishing targets and emerging targets during automatic tracking. The interested area was determined with the characteristics of the alignment axis of the microscope. The trend of cell movement is analyzed, and the feasibility of the algorithm is verified by automatic experimental research. The results demonstrate that the strategy proposed in this work can be of great significance for the virtual cell modeling, which plays a positive role in the realization of microbial transport mechanism, micro-cell segmentation technology, high-speed motion tracking and other aspects, making it widely used in biomedicine systems.

REFERENCES

[1] T. Yiping, J. Rongjian, and L. Lulu, "Obstacle detection method for mobile robot using active omnidirectional vision sensor," *Comput. Sci.*, vol. 42, no. 3, pp. 284–288, Mar. 2015.

[2] Z. Jiaxuan and W. Chengru, "A three resolution for obstacle detection using stereo vision," *Comput. Secur.*, vol. 10, pp. 9–12, Oct. 2010.

[3] A. Halawani, S. U. Réhman, and H. Li, "Active vision for tremor disease monitoring," *Procedia Manuf.*, vol. 3, pp. 2042–2048, 2015.

[4] J. M. Molina-Casado, E. J. Carmona, and J. García-Feijoó, "Fast detection of the main anatomical structures in digital retinal images based on intra- and inter-structure relational knowledge," *Comput. Methods Programs Biomed.*, vol. 149, pp. 55–68, Oct. 2017.

[5] M. P. Harris, E. Kim, B. Weidow, J. P. Wikswo, and V. Quaranta, "Migration of isogenic cell lines quantified by dynamic multivariate analysis of single-cell motility: Incomplete laminin processing exposes a tumor target," *Cell Adhesion Migration*, vol. 2, no. 2, pp. 127–136, 2008.

[6] J. Riedl *et al.*, "Lifeact mice for studying F-actin dynamics," *Nature Methods*, vol. 7, no. 3, pp. 168–169, 2010.

[7] Y. Kalaidzidis, "Intracellular objects tracking," *Eur. J. Cell Biol.*, vol. 86, no. 9, pp. 569–578, 2007.

[8] Z. Qinglian and Z. Xin, "Adaptive genetic algorithm with three parent crossover for numerical optimization," *J. Tianjin Normal Univ., Natural Sci. Ed.*, vol. 37, no. 5, pp. 55–59, May 2017.

[9] S. Mingzhu and G. Xianwei, "S. Mingzhu and G. Xianwei, "Parameters identification method via cepstrum analysis for mix blurred image restoration," *J. Tianjin Normal Univ., Natural Sci. Ed.*, vol. 37, no. 5, pp. 60–65, May 2017.

[10] Z. Xiu and Z. Zhihan, "Near-ELD plate applied in wireless power transmission system," *J. Tianjin Normal Univ., Natural Sci. Ed.*, vol. 37, no. 6, pp. 58–61, Jun. 2017.

[11] M. Chuai, D. Hughes, and C. J. Weijer, "Collective epithelial and mesenchymal cell migration during gastrulation," *Current Genomics*, vol. 13, no. 4, pp. 267–277, 2012.

[12] T. Bretschneider, H. G. Othmer, and C. J. Weijer, "Progress and perspectives in signal transduction, actin dynamics, and movement at the cell and tissue level: Lessons from Dictyostelium," *Interface Focus*, vol. 6, no. 5, p. 20160047, 2016.

[13] M. Pineda, C. J. Weijer, and R. Eftimie, "Modelling cell movement, cell differentiation, cell sorting and proportion regulation in Dictyostelium discoideum aggregations," *J. Theor. Biol.*, vol. 370, pp. 135–150, Apr. 2015.

[14] S. T. Johnston, M. J. Simpson, and R. E. Baker, "Modelling the movement of interacting cell populations: A moment dynamics approach," *J. Theor. Biol.*, vol. 370, pp. 81–92, Apr. 2015.

[15] N. Amariglio *et al.*, "Changes in gene expression pattern following granulocyte colony-stimulating factor administration to normal stem cell sibling donors," *Acta Haematol.*, vol. 117, no. 2, pp. 68–73, 2007.

[16] H. Shen *et al.*, "Automatic tracking of biological cells and compartments using particle filters and active contours," *Chemometrics Intell. Lab. Syst.*, vol. 82, nos. 1–2, pp. 276–282, 2006.

[17] W. Wei, J. Yu, and W. Dan, "Through wall human detection based on stacked de noising auto encoder algorithm," *J. Tianjin Normal Univ., Natural Sci. Ed.*, vol. 37, no. 5, pp. 50–54, May 2017.

[18] B. Mingshuai and M. Jiasong, "Application of convolutional neural network in vaccinated egg classification," *J. Tianjin Normal Univ. (Natural Sci. Ed.)*, vol. 38, no. 1, pp. 56–58, 2018.

[19] B. Mingshuai and M. Jiasong, "Application of convolutional neural net work in vaccinated egg classification," *J. Tianjin Normal Univ., Natural Sci. Ed.*, vol. 38, pp. 56–58, Jan. 2018.

[20] T. Yi, L. Wei-Ming, and X. Liang, "Improving robustness and accuracy in moving object detection using section-distribution background model," in *Proc. 4th Int. Conf. Natural Comput.*, Oct. 2008, pp. 167–174.

[21] J. J. Corso, E. Sharon, S. Dube, S. El-Saden, U. Sinha, and A. Yuille, "Efficient multilevel brain tumor segmentation with integrated Bayesian model classification," *IEEE Trans. Med. Imag.*, vol. 27, no. 5, pp. 629–640, May 2008.

[22] R. M. Jiang, D. Crookes, N. Luo, and M. W. Davidson, "Live-cell tracking using SIFT features in DIC microscopic videos," *IEEE Trans. Biomed. Eng.*, vol. 57, no. 9, pp. 2219–2228, Sep. 2010.

[23] D. R. Magee, "Tracking multiple vehicles using foreground, background and motion models," *Image Vis. Comput.*, vol. 22, no. 2, pp. 143–155, 2004.

[24] S. Dash, A. Verma, C. North, and W.-C. Feng, "Portable parallel design of weighted multi-dimensional scaling for real-time data analysis," in *Proc. IEEE Int. Conf. High Perform. Comput. Commun., IEEE Int. Conf. Smart City, IEEE Int. Conf. Data Sci. Syst.*, Dec. 2017, pp. 10–17.

[25] H. Y. N. Holman, M. C. Martin, and W. R. Mckinney, "Tracking chemical changes in a live cell: Biomedical applications of SR-FTIR spectromicroscopy," *Spectroscopy*, vol. 17, nos. 2–3, pp. 139–159, 2014.

[26] F. Kong and J. Tan, "DietCam: Regular shape food recognition with a camera phone," in *Proc. IEEE Int. Conf. Body Sensor Netw.*, May 2011, pp. 127–132.

[27] M. Muja and D. G. Lowe, "Fast approximate nearest neighbors with automatic algorithm configuration," in *Proc. Int. Conf. Comput. Vis. Theory Appl.*, 2009, pp. 331–340.

[28] D. G. Lowe, "Distinctive image features from scale-invariant keypoints," *Int. J. Comput. Vis.*, vol. 60, no. 2, pp. 91–110, 2004.

[29] J. Mutch and D. G. Lowe, "Object class recognition and localization using sparse features with limited receptive fields," *Int. J. Comput. Vis.*, vol. 80, no. 1, pp. 45–57, 2008.

[30] E. Hamuda, B. M. Ginley, M. Glavin, and E. Jones, "Improved image processing-based crop detection using Kalman filtering and the Hungarian algorithm," *Comput. Electron. Agricult.*, vol. 148, pp. 37–44, May 2018.

XIN YIN was born in Tianjin, China. She received the B.S. and M.S. degrees in computer science from Tianjin Normal University, and the Ph.D. degree in control theory and engineering from the Robotics and Information Automation Institute, Nankai University, in 2006.

She has been with the School of Physics and Electronic Information, Tianjin Normal University, since 2003. Her research interests are artificial intelligence and pattern recognition, such as the sensor tracking with micro-operation.

She became an Associate Professor in 2007. In 2009, she was with Dundee University, U.K., as a Visiting Scholar. She has published many important research papers on pattern recognition under micro-operation.

GUONAN JIANG is currently pursuing the degree with the School of Physics and Electronic Information, Tianjin Normal University.

In 2018, she became a member of the Excellent Student Program.

SHIDONG SONG was born in Tianjin, China. He received the B.S. and M.S. degrees from Nankai University and the Ph.D. degree from Tianjin University.

He is currently a Professor at Tianjin Polytechnic University.

He was selected as the New Century Excellent Talents in China Universities in 2010 and has published many important papers.

• • •